Magnetism in finite-sized single-walled carbon nanotubes of the zigzag type

Jianhua Wu
Computational Center for Molecular Structure and Interactions, Department of Physics, Atmospheric Sciences, and Geoscience, Jackson State University, Jackson, Mississippi 39217, USA

Frank Hagelberg
Department of Physics and Astronomy, East Tennessee State University, Johnson City, Tennessee 37614, USA
(Received 21 October 2008; revised manuscript received 11 February 2009; published 26 March 2009)

The magnetic properties of (10,0) finite-sized single-walled carbon nanotubes (SWNTs) have been investigated by use of density-functional theory. A comparative study on the impact of different nanotube terminating structures on the magnetic states of these systems is presented. Three termination modes are included: hydrogenation, truncation with edge reconstruction, and capping by fullerene hemispheres. Magnetic ground states are reported for all systems considered. The magnetic moments of truncated and hydrogenated systems were found to localize at the SWNT ends, with preference for antiparallel orientation, or antiferromagnetic order. Capped systems, in contrast, exhibit a delocalized spin-density distribution as well as a tendency toward ferromagnetic order beyond a critical length. The magnetic phenomena described here are attributed to edge effects associated with the reduction in periodic SWNTs to finite size. The spin densities of the considered SWNTs are investigated as a function of their lengths, and an analogy between the resulting structures and the magnetization induced in a nonmagnetic metal inserted into an environment with itinerant magnetism is outlined.

DOI: 10.1103/PhysRevB.79.115436 PACS number(s): 75.75.+a, 61.48.De, 81.07.−b, 75.50.−y

I. INTRODUCTION

Carbon nanotubes (CNTs) have attracted much attention since their discovery in 1991.[1,2] In particular, single-walled carbon nanotubes (SWNTs) have been shown to hold great promise for potential applications in nanodevices.[3–6] SWNTs may be metallic, quasimetallic, or semiconducting, as determined by the tubular circumferential vector or chiral vector $\mathbf{C}_h = n\mathbf{a_1} + m\mathbf{a_2} \equiv (n,m)$ that connects crystallographically equivalent sites on a two-dimensional graphene sheet. As demonstrated by calculations involving periodic boundary conditions, the metallic or semiconducting nature of SWNTs is governed by two parameters, namely, the chiral angle and the tube diameter.[7–9]

Recent attention has focused on SWNTs of finite length[10–14] for both their fundamental and technological interest. Potential applications of these units range from molecular electronics to medical diagnostics involving nanopharmaceuticals. Thus, finite metallic nanotubes may be employed as microscopic conducting elements as they are connected to leads which may be chosen as metal clusters or nanotubes themselves. A very different potential application of these systems exploits their cage structure for confining clusters of lanthanide atoms.[10] The resulting composites have been experimentally shown to display unprecedented proton relaxation efficiency, making them interesting candidates for novel contrast agents in magnetic-resonance imaging (MRI).

The geometric and electronic properties of SWNTs change dramatically as they are reduced to finite length. By the example of the case $m=n=5$, it has been demonstrated that the energy gaps of finite-length nanotubes of the armchair type ($m=n$) exhibit oscillatory decrease as a function of the tube length.[11–14] The energy gaps of finite-length metallic nanotubes of the zigzag type ($m=0$), in contrast, decrease monotonically with the SWNT length,[11,12] as was shown for the case of the (9,0) system.

Recent research has highlighted the critical impact exerted by the tube edges on the properties of the nanotube.[15–28] The electronic structure of these edges is strongly determined by the nature of the nanotube. From density-functional theory (DFT) studies[15] of hydrogenated SWNTs, localized states at the tube edges were identified for systems of the zigzag, but not of the armchair type. This effect, in turn, is responsible for the appearance of magnetism in hydrogenated zigzag SWNTs.[16–18] Likewise, a magnetic ground state has been reported for truncated zigzag SWNTs, i.e., cylindrical segments of the respective periodic systems, with n varying from 4 to 14.[18] SWNT species with different terminating structures at the two tube ends have been explored for very short systems comprising six atomic layers.[19] Here, one end was truncated while the other one was terminated by either a ring of H atoms or a fullerene hemisphere. In all cases examined, DFT computation led to the prediction of a magnetic ground state. A finite spin up to $S=2$ has been reported for (7,0) and (8,0) SWNTs with mixed monohydrogenated and dihydrogenated edge atoms.[20]

We point out that these observations manifest a phenomenon that is not limited to zigzag SWNTs but may be encountered in other carbon nanostructures as well,[17–27] such as finite graphene sheets which may be interpreted as unrolled SWNTs of the zigzag type, so-called *zigzag graphene nanoribbons* (ZGNRs), further fullerenes with Stone-Wales defects,[19] or carbon nanotubes with vacancies, nonmetal impurities, or line defects. For these systems, magnetic order has been predicted to occur even in the absence of transition-metal impurities. ZGNRs as well as zigzag SWNTs have been characterized as half metals, as in both cases the electronic gap is found to be zero for one spin orientation but not for the other as the studied nanosystem is exposed to an electric field of critical strength.[17,18,28–30]

Further, the emergence of magnetism in proton-irradiated thin carbon films[24,25] and nanodiamonds implanted with ^{15}N and ^{12}C ions[26] has recently been proven experimentally. As demonstrated by soft x-ray absorption microscopy,[24] the ferromagnetic order induced in proton-irradiated carbon films is not caused by any hydrogen admixtures but originates only from carbon π electrons.

In all presently available studies of zigzag SWNT magnetism, nonzero magnetic moments were found to be associated with localized edge states. Both truncation and monohydrogenation of these systems give rise to undercoordinated trivalent carbon atoms at the zigzag edges, while any globally saturated configuration of the carbon network involves tetravalent bonding of each atom, corresponding to the presence of one double and two single bonds.[16] The prevalence of magnetic solutions for finite zigzag nanotubes appears thus correlated with the emergence of unpaired electronic states localized at the tube ends. The local magnetic moments may adopt parallel or antiparallel orientation with respect to each other, or, loosely speaking, arrange in ferromagnetic (FM) or antiferromagnetic (AFM) order. Presently available computational studies suggest higher stability of the latter phase as compared with the former in case of symmetric capping of both ends.[17,18] Kim *et al.*,[19] however, arrived at the prediction of FM order for short $(n,0)$ units with $n=8$, 10 if one tube end is saturated with a fullerene hemisphere and the other left open.

A detailed understanding of SWNT magnetism appears not only to add an important facet to our knowledge of fundamental nanotube features but also to open a perspective on the use of these systems in nanotechnological applications. Specifically, it is expected that the transport properties of finite SWNTs are influenced by their magnetic characteristics, making the systems discussed here promising candidates for future spin-based electronic nanodevices.[31]

This contribution aims at a systematic investigation of finite zigzag SWNT magnetism as a function of various basic structural parameters. By the example of the (10,0) system, we study the electronic structure as well as the magnetic order emerging in SWNTs of varying length and, most importantly, with different structures terminating the tube ends. The comparative stabilities of the competing magnetic phases will be discussed along with the spatial distribution of the electronic magnetic-moment densities. The question to what extent the magnetic properties of zigzag SWNTs can be defined by controlling elementary parameters pertaining to nanotube architecture will receive particular attention in view of its relevance for the possible nanotechnological utilization of these systems.

II. COMPUTATIONAL DETAILS

The results presented in this contribution were obtained mostly by DFT employing a plane-wave basis set[32] as implemented by the Vienna *ab initio* simulation package (VASP).[33,34] The finite temperature version of local-density functional (LDF) theory[35] was utilized in conjunction with the exchange-correlation functional given by Ceperley and Alder and parameterized by Perdew and Zunger.[36] The generalized Kohn-Sham equations[32] are solved utilizing the residual metric minimization with direct inversion in the iterative subspace (RMM-DIIS) method.[37,38] The optimization of the atomic geometry is performed via conjugate-gradient minimization of the total energy with respect to the atomic coordinates. Instead of Fermi-Dirac broadening of the one-electron energies, it may be computationally convenient to choose Gaussian broadening which was employed in this work. The width of the Gaussian distribution was selected as 0.001 eV. The total energy of the system refers to the limit of vanishing width.

The interaction of valence electrons and core ions is described by the projector-augmented wave (PAW) method.[39] All DFT calculations involved the generalized gradient correction (GGA) for the exchange-correlation functional as prescribed by Perdew, Burke, and Ernzerhof.[40]

Periodic boundary conditions were imposed on a cubic cell with dimension $20\times20\times d_z$ Å^3. The parameter d_z depends on the length of the chosen nanotube. In each individual case, it was chosen sufficiently large to minimize the interaction between neighboring systems. From inspection of the converged equilibrium geometries, the nearest-neighbor distance between atoms in adjacent supercells is larger than 12 Å, making the interaction between supercells negligible. Finally, the geometry was optimized enforcing a difference of less than 1 meV between the total energies obtained in two subsequent steps as convergence criterion. In some selected cases, comparison was made with the results of quantum chemical calculations employing the B3LYP potential in conjunction with the 3–21 G basis set.[41]

III. RESULTS

In the following, we will discuss (10,0) SWNTs differing with respect to length and terminating structures. After introducing in Sec. III A the systems considered, we will focus first on their geometric structure (Sec. III B) and then on their electronic and magnetic properties (Sec. III C).

A. Systems studied

Three prototypes of finite-sized (10,0) SWNTs are considered in this work. As shown in Figs. 1(a)–1(c), they differ with respect to the tube-terminating structures. More specifically, we distinguish between (a) SWNTs with hydrogen termination [Fig. 1(a)], (b) truncated SWNTs where admission is made for geometric reconstruction of the tube ends [Fig. 1(b)], and (c) SWNTs saturated by capping with fullerene hemispheres [Fig. 1(c)]. In cases (a) and (c), each carbon atom in the nanotube top or bottom layer has one or two dangling bonds which are partially or completely saturated by the added H atoms or fullerene fragments, respectively. In case (b), another edge saturation mechanism is operative. Truncation involves the breaking of the C-C bonds between the two layers that form the trans-polyene chain [Fig. 1(b)]. As a consequence, each top (bottom) C atom has two or three dangling bonds. As the ten C atoms in the top (bottom) layer reconstruct, each atom in these layers forms bonds with its two nearest neighbors, establishing the maximally achiev-

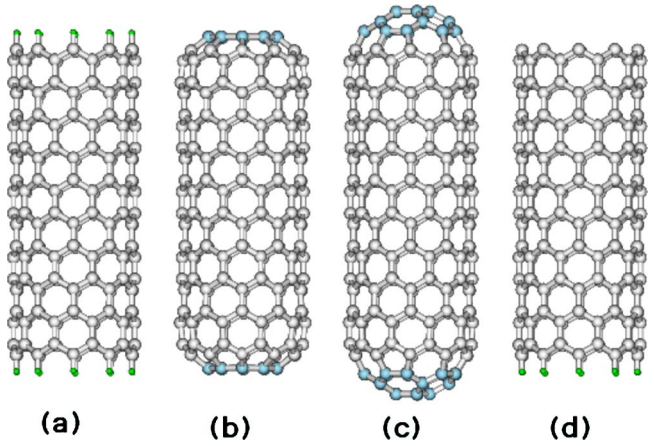

FIG. 1. (Color online) The equilibrium geometries of a (10,0) SWNT with $L=10$ and (a) H termination, (b) truncation with reconstructed edge layers, (c) capping with fullerene hemispheres, and (d) asymmetric termination with one end hydrogenated and the other one truncated. Green (small) symbols represent H, and gray symbols C atoms of intermediate layers, while light blue (dark) symbols indicate C atoms in the terminating decagons (b) or fullerene hemispheres (c).

able degree of saturation in both edge layers. We find the total ground-state energies of symmetrically truncated and reconstructed SWNTs with lengths $L=3,6,10$ by 23.135, 24.888, and 25.116 eV more stable than the respective open-ended systems. The length (L) is defined as the number of trans-polyene chains of the SWNTs.

For each one of the three nanotube types illustrated in Figs. 1(a)–1(c), we explore SWNTs of at least thirteen different lengths. The SWNT lengths as given in the following refer to the uncapped case. For the reconstructed case, the decagon rings at the top and the bottom of the SWNT are not included in the indicated number of layers.

In addition, we consider the case of asymmetric capping, involving one H terminated and one truncated tube end. In this configuration, truncation was performed between trans-polyene chains and thus did not lead to reconstruction.

B. Geometric properties

In this section, we present our results pertaining to structural features of the studied (10,0) SWNTs with the three different edge arrangements described above. Commenting first on H-terminated SWNTs, we find that the trans-polyene chains, i.e., the zigzag-structured rings that form the SWNT circumference, are characterized by equidistant C-C bonds. For a SWNT of length $L=10$, as shown in Fig. 1(a), this bond length decreases from 1.430 Å at the center layer to 1.416 Å at the top (bottom) layer. In the direction of the tube axis, the C-C bond length increases from 1.423 Å at the tube center to 1.440 Å at the top layer. These values agree with those reported for the (9,0) SWNT.[12]

In the case of a truncated SWNT, the carbon atoms in the top (bottom) layer, forming a regular decagon, bend toward the tube center. Each atom bonds with two neighbors in the same layer. The distance between next neighbors within the decagon is determined to be 1.451 Å for the SWNTs included here except for the shortest SWNT ($L=1$). The bond length connecting the top (bottom) of the nanotube to the adjacent layer increases from 1.424 Å for the periodic species to 1.503 Å for the SWNT with $L=20$.

The C-C distances within the trans-polyene chains close to the top (bottom) are 1.390 Å for the SWNT with $L=20$ and thus markedly shorter than in the periodic SWNT. These distances elongate slightly, namely, by 0.006 Å as one goes from $L=20$ to $L=2$. The bond length along the tube axis decreases by the same margin from the ends to the SWNT center. A more marked distortion is recorded for shorter SWNTs.

Turning to the case of fullerene capping, we encounter a distinct pattern of C-C bond-length variation within the trans-polyene chains. Neither are these bond lengths equal to each other, as they are in the periodic species, nor do they display a characteristic long-long-short alternation as in the case of (9,0) SWNTs.[12] In the (10,0) system, the C-C bonds connected to a cap pentagon are elongated, while those connected with a cap hexagon are shortened [see Fig. 1(c)]. Consequently, the tube axis parallel C-C bonds attaching to a pentagon (hexagon) motif of the cap structure shorten (elongate).

The terminating structure exerts a marked impact on the properties of the nanotube. Section III C will highlight the role of the termination mode in defining the electronic and magnetic features of the SWNTs studied in this work.

C. Electronic and magnetic properties

We comment here on our findings related to the magnetic moments, magnetic interaction strengths, stabilities, and energy gaps of (10,0) SWNTs with various symmetric and asymmetric termination structures in both the FM and the AFM states. Before discussing the case of symmetric edge termination, we comment on the asymmetric case which is discussed in Ref. 19 for extremely short (8,0) and (10,0) systems with length $L=3$. As a test, we compared the symmetrically truncated species with those truncated at one end and H terminated at the other, as shown in Fig. 1(d), for systems with $L=3,6$, and 10. As for the corresponding $L=3$ system described in Ref. 19, truncation is here performed by applying a cut between two adjacent trans-polyene chains, and the C atoms that form the SWNT edge do not rearrange in the course of geometry optimization.

For both types of SWNTs, we identified ferromagnetic as well as antiferromagnetic solutions, as summarized in Table I. The magnetic moments listed in the table, as obtained by integration of the magnetic-moment density, are largely located in the top and bottom regions of the nanotube. As seen from the results related to the comparative energies of the two competing phases, our computations yield an antiferromagnetic ground state in all cases considered. In agreement with Kim *et al.*,[19] we find a total magnetic moment of 10 a.u. for the asymmetric system with $L=3$. We arrive, however, at an AFM ground state for this species, which is favored over the FM alternative by an energy difference of 225 meV, while in Ref. 19 preference of the FM solution by a very

TABLE I. Magnetic moments, energy differences between FM and AFM spin configurations for SWNTs (L=3, 6, and 10) with one open and one H-terminated end as well as with both ends left open.

	μ (μ_B)						
	FM			AFM			$E_{FM}-E_{AFM}$
System	Left	Right	Total	Left	Right	Total	(eV)
L=3 hydrogenated	11	1	12	12	−2	10	0.225
L=6 hydrogenated	13	3	16	13	−3	10	0.058
L=10 hydrogenated	13	3	16	13	−3	10	0.011
L=3 open ended	11	11	22	12	−12	0	0.719
L=6 open ended	13	13	26	13	−13	0	0.074
L=10 open ended	13	13	26	13	−13	0	0.016

similar energy margin (275 meV) is reported. It should be noted that an AFM ground state was also found in the recent study of Mananes *et al.*[16] for symmetrically H-terminated (14,0) SWNTs with L=4 and 6. For the L=3 (10,0) SWNTs with two open ends, we observe a strong preference of the AFM state. This agrees qualitatively with the result of Kim *et al.*,[19] while the energy difference between FM and AFM states as obtained from our calculations deviates slightly from that indicated in Ref. 19.

Insight into the origin of the observed magnetic effects is gained from inspecting the SWNT spin-density distribution. For representing this quantity, the spin-density profile along the tube axis was integrated over the tube radius and azimuthal angle in Figs. 2 and 3 for the cases of L=3 and 6. From Fig. 2, the spin density is markedly higher at the truncated tube end than at the hydrogen-terminated end. By further integrating the spin density over the left and right regions of the tube axis, we obtain the top and bottom magnetic moments indicated in Table I. In each case, the magnetic moment assigned to the left (right) half of the SWNT is obtained from integrating the spin density from the middle layer to the respective end of the system.

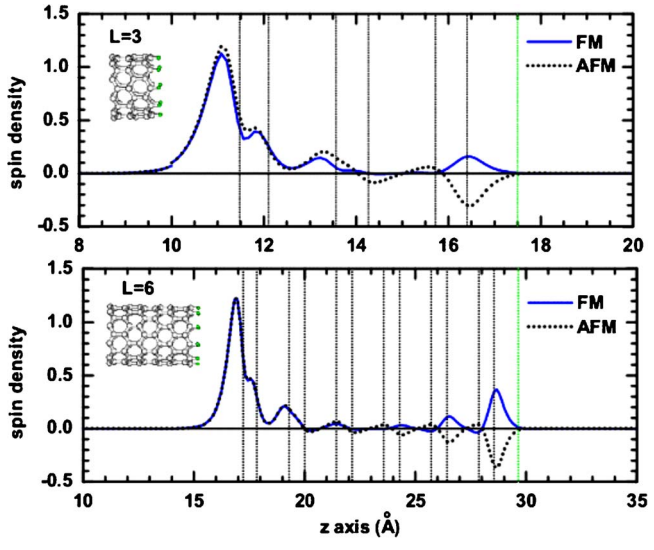

FIG. 2. (Color online) Spin-density distribution along the tube axis (z axis) for SWNTs (L=3,6) with one H-terminated and one open end. The dotted perpendicular lines indicate the position of carbon and hydrogen atoms. The line on the outermost right [green color (light in print)] refers to the terminating H layer. The left edge is open ended, in accordance with the labels used in Table I.

Clearly, the dominant contributions to the overall magnetic moment stem from the tube edges. The resulting magnetic moments of this s-p electron system can thus be attributed to the localization of unpaired electrons at the edges of the considered complex, in close analogy to respective results on zigzag graphene ribbons.[21] For proton irradiated thin carbon films, the origin of magnetism from carbon π electrons has been confirmed experimentally.[24] The spin density displays an oscillatory behavior as a function of the tube length, where the oscillation amplitude reduces from its maximum value to zero as one goes from the edges to the tube center. This pattern is comparable to that of the magnetization induced in a nonmagnetic (NM) metal layer as it is attached to a layer with itinerant magnetism.[42] As shown by a simulation based on the single-band Hubbard model,[43] the magnetization imposed on the nonmagnetic segment by its ferromagnetic environment gives rise to a long-range de-

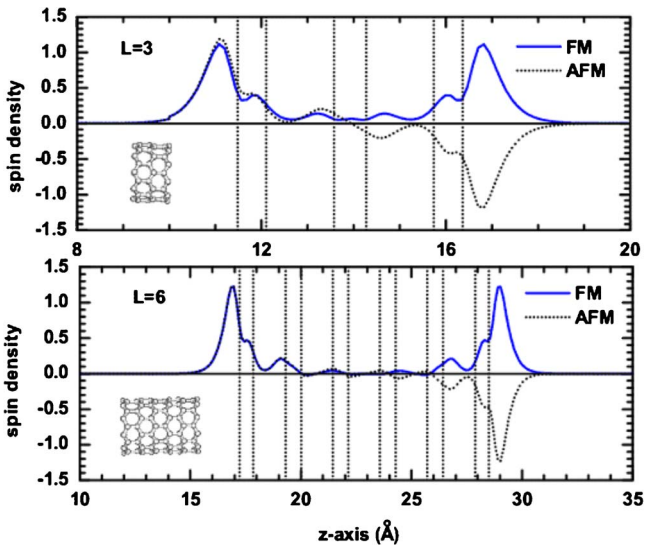

FIG. 3. (Color online) Spin-density distribution along the tube axis for L=3 and 6, where both SWNT ends are left open. The dotted perpendicular lines indicate the position of the C atoms.

creasing oscillation as a function of the length coordinate of this segment. In this simulation, the on-site Coulomb interaction vanishes in the nonmagnetic segment. The electrons in this segment may therefore be compared to the *s* and *p* electrons in the middle part of the SWNTs. The localized unpaired electrons at the SWNT edges create magnetic boundary conditions and so exert a spin polarizing effect on the delocalized π electrons inside the SWNT which therefore behave like uncorrelated electrons in nonmagnetic metals.

We point out that spin-density oscillations have been shown to occur in quantum wires where they are caused by spin-orbit interaction.[44] From recent theoretical work on spin-orbit coupling in curved carbon nanostructures,[45] we extrapolate the size of this effect to be in the order of 2 meV. Further, spin-density oscillations induced in quantum wires by spin-orbit coupling have been shown to be constant in amplitude. Thus, the essential features of the distributions shown in Figs. 3, involving maxima at the tube edges and minima at the tube centers, are not expected to be markedly changed upon incorporation of the spin-orbit effect.

It should be noted that even if the magnetic coupling between both ends is antiferromagnetic, the total magnetic moments are not zero in case of the asymmetric system, involving an H-terminated and an open tube end. This is plausible as the local magnetic moment of the latter distinctly exceeds that of the former.

We turn now to the systems displayed in Figs. 1(a)–1(c), having symmetric edge structures, and place emphasis on the effect of the tube ends on the magnetism of the considered species. Table II summarizes the main results obtained on the three SWNT prototypes compared here. Each of these species was investigated in FM as well as AFM order. The overall magnetic moment of the FM phase was recorded as a function of the tube length, along with the energy gap for both the FM and the AFM system, the energy difference between both magnetic states, and the magnetic coupling in the ground state.

The magnetic and electronic properties of symmetrically H-terminated and truncated SWNTs turn out to be quite similar. From our calculation, ultrashort SWNTs with $L=1$ and 2 are nonmagnetic. For all three SWNT types, the magnetic moment is seen to reach its asymptotic value at the length of $L=4$. This value is 6 a.u. for H-terminated and truncated systems in the FM state, in agreement with the findings related to the asymmetric units discussed above (see Table I), where the magnetic moment at H-terminated edges was found to be 3 a.u. The AFM phase is most stable throughout in the case of H-terminated and truncated SWNTs.

For hydrogenated systems with $L=4$, 6, and 8 we find the same order of energy differences $E_{\mathrm{FM}}-E_{\mathrm{AFM}}$ as Du *et al.*[18] This quantity is substantially higher for the shortest of these three units than for the others. Also, our results confirm the overall trend of the differences $E_{\mathrm{NM}}-E_{\mathrm{GND}}$ reported in Ref. 18, involving the AFM ground state as compared with the NM state. Here, the result for the shortest of the three SWNTs is markedly smaller than that for the two longer ones. While the qualitative agreement of our findings with those presented in Ref. 18 is good, the magnitudes of the energy differences indicated there are consistently by about a factor of 2 lower than those shown in Table II.

While AFM ordering prevails for hydrogenated and truncated systems, the FM and AFM phases are almost degenerate for capped SWNTs, where an upper bound on the energy difference between these two magnetic states is given by 10 meV. The asymptotic magnetic moment in the ferromagnetic state is here 2 a.u.. The AFM phase is most stable for the capped systems as well, except for the SWNTs with $L=5$, and those longer than $L=14$. Asymptotically, the FM phase becomes the most stable solution.

Inspecting the magnetic distributions in detail, we plot the axial magnetic density profile along the tube axis for H-terminated, truncated, and capped SWNTs with $L=10$, as well as a capped SWNT with $L=18$ (Fig. 4). For the two former SWNT types, sp^2 termination prevails.[16] In H-terminated SWNTs, the top (bottom) C atoms form σ bonds with H atoms, and the π electron density piles up at the top (bottom) layer of the tube. In truncated SWNTs, however, both σ and π electrons of C atoms at the top (bottom) tube layer connect with those of the terminating decagon ring. Consequently, one finds the electrons in the H-terminated SWNTs more sharply localized than those in the truncated SWNTs, as is evident from comparing the dominant maxima of the corresponding profiles shown in Figs. 4(a) and 4(b).

The spin-density profile of the $L=10$ capped SWNT adopts large values at the limiting pentagon rings of the terminating caps [Fig. 4(c)]. As both the top and the bottom layer of each capping hemisphere consist of a pentagon, i.e., of five C atoms only [see Fig. 1(c)], the spin density per C atom is largest for these layers. This implies localization of the electrons on the capping pentagon rings, inducing a magnetic moment at the top of the SWNT caps. In addition, from Fig. 4(c), the spin density is found to be large at the interface between the cap and the tube. As a characteristic structural feature, the interface region exhibits a regular arrangement of alternating pentagons and hexagons. The cap and the tube segments are connected by σ bonds shared by adjacent pentagons and hexagons, inducing π electron localization at the C atom layers neighboring the capping hemispheres. Turning to the longer capped SWNT with $L=18$ [see Fig. 4(d)], the spin-density profile is seen to differ sensitively from that of the shorter unit. The changes between both distributions can be summarized into two key features: the profile becomes more regular and more delocalized. The maxima are shifted toward the tube center, with their peak values gradually reducing to zero from the interface to the central region of the tube.

The magnetic densities characteristic of the capped SWNTs are about an order of magnitude below those present in H-terminated and truncated SWNTs, reflecting a much lower degree of electron localization in case of capped SWNTs. In geometric terms, the fullerene hemispheres release the edge contraction typical for the two alternative structures, corresponding to a less strained SWNT termination.

In the H-terminated and truncated cases, the energy difference between the FM and the AFM phases decreases monotonically with increasing tube length. A reduction to 4 meV is found in the $L=20$ unit, the longest SWNT included in this comparison. At this tube length, the FM and AFM

TABLE II. Magnetic and electronic properties of symmetrically terminated (10,0) SWNTs, comprising H-terminated, open reconstructed, and capped SWNTs. The symbol μ_{FM} refers to the magnetic moment of the FM state.

Systems	Length	μ_{FM} (μ_B)	E_{gap} (eV)		$E_{FM}-E_{AFM}$ (eV)	$E_{NM}-E_{GND}$ (eV)
			FM	AFM		
H-terminated	1	0[a]		0.645[a]		
	2	0[a]		0.640[a]		
	3	2	0.398	0.696	0.172	0.379
	4	6	0.223	0.688	0.274	0.480
	5	6	0.398	0.631	0.103	0.759
	6	6	0.498	0.609	0.048	0.878
	7	6	0.539	0.601	0.026	0.937
	8	6	0.565	0.599	0.018	0.960
	9	6	0.579	0.598	0.013	0.973
	10	6	0.585	0.596	0.010	1.094
	11	6	0.587	0.593	0.008	0.986
	12	6	0.591	0.594	0.007	1.000
	20	6	0.591	0.591	0.004	0.994
Truncated	1	0[a]		0.318[a]		
	2	0[a]		0.491[a]		
	3	2	0.379	0.587	0.128	0.315
	4	6	0.151	0.568	0.176	0.386
	5	6	0.316	0.526	0.093	0.716
	6	6	0.389	0.502	0.042	0.725
	7	6	0.428	0.491	0.026	0.812
	8	6	0.453	0.490	0.014	0.845
	9	6	0.469	0.487	0.010	0.824
	10	6	0.476	0.482	0.008	0.834
	11	6	0.478	0.485	0.007	0.877
	12	6	0.483	0.486	0.006	0.832
	20	6	0.486	0.486	0.004	0.813
Capped	1	0[a]		0.116[a]		
	2	0[a]		0.132[a]		
	3	0[a]		0.079[a]		
	4	2	0.062	0.095	0.006	0.025
	5	2	0.084			0.019
	6	2	0.081	0.097	0.003	0.055
	7	2	0.063	0.095	0.010	0.037
	8	2	0.107	0.107	0.002	0.086
	9	2	0.100	0.113	0.003	0.075
	10	2	0.116	0.119	0.006	0.080
	11	2	0.086	0.094	0.002	0.063
	12	2	0.073	0.077	0.003	0.071
	13	2	0.039	0.054	0.007	0.047
	14	2	0.028	0.035	−0.003	0.028
	15	2	0.045			0.029
	20	2	0.065			0.031

[a]No magnetic phase has been identified.

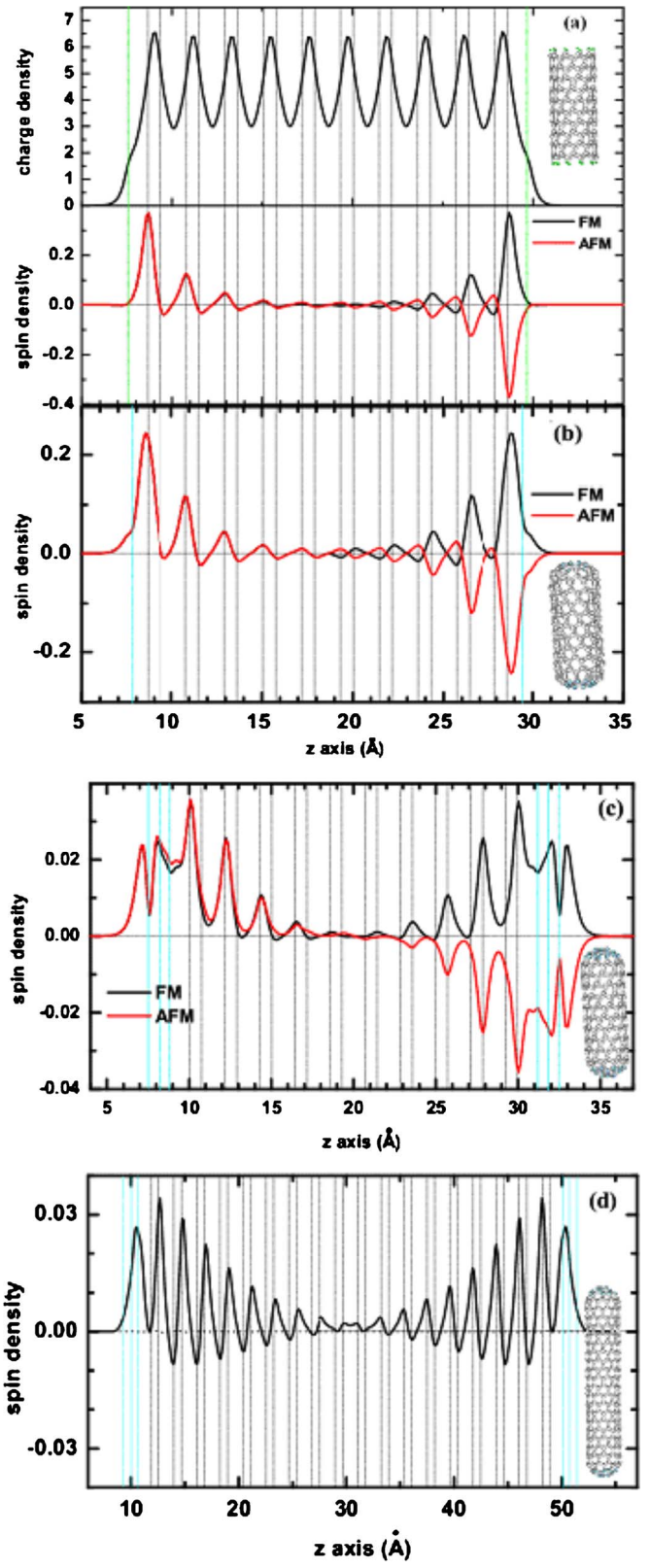

FIG. 4. (Color online) Charge and spin densities for a $L=10$ (a) H-terminated, (b) truncated, (c) capped, and (d) $L=18$ capped SWNT. The perpendicular lines indicate the positions of the H or C atom layers. In (b)–(d), the C atom layers of the reconstruction or capping regime are indicated by light blue lines (light gray in print).

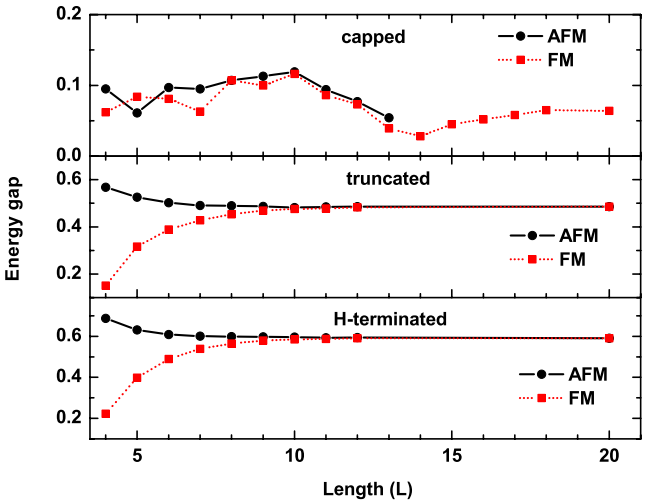

FIG. 5. (Color online) Energy gap as a function of nanotube length for H-terminated, truncated, and capped SWNTs including FM and AFM states.

states are nearly degenerate. Consequently, a suitably applied magnetic field should be able to alter the magnetic state from AFM to FM in this case. The transport properties are found to diminish upon the change in the magnetic state from FM to AFM in magnetic multilayers.[46,47] In view of the very small energy margin separating the FM state from the ground state, metastability is expected for the FM phase with a lifetime sufficiently long to exploit the respective large magnetic moment for practical applications. These may comprise the use of the SWNTs discussed here as magnetoresistive materials and nonmetal magnetic devices. We also point out that the high degree of localization of edge states with opposite spin polarization in hydrogenated and truncated SWNTs draws a close parallel between these systems and ZGNRs, which have been characterized as promising candidates for spintronics applications.[18,28] Under this viewpoint, examining the systems considered here for half-metallicity features will be of interest.

The energy gaps are defined as the difference between the highest occupied and the lowest unoccupied energy level, irrespective of spin orientation. They are found to narrow as the tube length increases for AFM states of H-terminated and truncated SWNTs. The opposite tendency is observed for FM states. Asymptotically, the energy gaps for both magnetic phases converge, as demonstrated in Fig. 5. The calculated energy gap for a $L=20$ H terminated SWNT is 0.591 eV, and 0.486 eV for a truncated SWNT of the same length. Experimentally, the energy gap of the (10,0) SWNT has been determined to be 1.1 eV.[4] In a separate computation on the periodic (10,0) SWNT, we found a value of 0.89 eV. The agreement between the theoretical and the experimental findings might be deemed satisfactory, considering that DFT tends to underestimate molecular energy gaps.[48] Once more, the behavior of the capped SWNT is seen to differ from that of the two other prototypes. Here, the energy gap decreases in an oscillatory mode with the increase in the SWNT length. This trend deviates from that found for the (9,0) system, where the gap decreases monotonically.[12]

For confirmation of our prediction of SWNT ground-state magnetism, quantum chemical computations at the B3LYP/

3–21G level were performed for the H-terminated SWNT with $L=4$ as test system. Geometry optimizations were performed with the spin multiplicities 1, 3, 5, 7, and 9. The magnetic states obtained turned out to be consistently lower than the respective nonmagnetic phases. While the applied quantum chemical procedure does not allow for optimization of an AFM state, we find the FM state with the magnetic moment $m=6\mu_B$ to be maximally stable, in accordance with the respective entry in Table I. From quantum chemical computation, this magnetic ground state exceeds the spin singlet alternative by a stability margin of 0.958 eV.

IV. CONCLUSION

Finite-sized zigzag SWNTs of the (10,0) type have been investigated by DFT with respect to their geometric, energetic, electronic, and magnetic properties, with emphasis on the dependence of these properties on the mode of nanotube termination. Three termination prototypes were considered: Hydrogenation, truncation with edge reconstruction, and capping by fullerene hemispheres. The evolution of the magnetic features of these types with increasing SWNT length was studied for systems varying in length from $L=1$ to 20. Further, we inspected the case of asymmetric termination by including (10,0) systems with one end hydrogenated and the other left open.

Magnetic ground states were found for all species investigated. The hydrogenated as well as the truncated units exhibit AFM ordering throughout, involving antiparallel magnetic moments which are localized at the tube edges. This configuration is associated with the presence of unpaired electronic edge states and thus with the incomplete saturation of dangling C atom bonds by a single layer of H atoms or by C atom reconstruction following truncation. However, ground-state magnetism appearing as the infinite $S=0$ SWNT is reduced to finite length is not necessarily associated with the emergence of *localized* edge states. This is demonstrated by our results on capped systems beyond a critical length of $L=14$. In contrast to the two other prototypes discussed here, these systems display a delocalized magnetic density distribution along the tube axis. Further, no unanimous dominance of AFM ordering is recorded in this case. On the contrary, capped (10,0) SWNTs were found to exhibit FM ground states in the asymptotic length limit. The energy separation between the FM and the AFM phase, as well as between the magnetic and the nonmagnetic solution, turned out to be markedly lower than in the cases of hydrogenation or truncation. The two latter types can be understood in analogy to a composite involving a nonmagnetic metal surrounded by two layers with itinerant magnetism. In both arrangements, the respective middle segment mediates the magnetic interaction between system boundaries, while the magnetization induced in this region is strongly damped. For SWNT termination with fullerene hemispheres, however, this analogy breaks down. Here the magnetization penetrates into the intermediate regime, extending far beyond the ends of the tube. The near-degeneracy of the FM and AFM alternatives in the capped SWNTs studied in this work might make these systems suitable for use as magnetoresistive elements.

In continuation of this research, a comparative study between hydrogenated as well as truncated SWNTs and ZGNRs as a function of length is planned, under both a systematic and a practical viewpoint. ZGNRs have been described in the framework of the Hubbard model.[43,49] Employing this formalism for SWNT analysis will make it possible to define conditions for the appearance of antiferromagnetic coordination of the SWNT edge state by use of Lieb's theorem.[50]

Further, various current experimental efforts aim at fabricating extremely short SWNTs.[51] Once avenues for controlled manufacturing of these systems have been described, it will be of great nanotechnological interest to explore their potential use in molecular spintronics. Investigating the systems considered here with respect to half-metallicity will add information of relevance for these applications.

ACKNOWLEDGMENTS

This work is supported by the DoD through the U.S. Army/Engineer Research and Development Center (ERDC, Vicksburg, MS) Contract No. W912HZ-06–C-005, and by the East Tennessee State University/Research Development Committee (ETSU/RDC) Grant No. RD0084. All computations have been performed on the Cray XT3 machine Sapphire machine at the ERDC.

[1] S. Iijima, Nature (London) **354**, 56 (1991).
[2] S. Iijima and T. Ichihashi, Nature (London) **363**, 603 (1993).
[3] J. C. Charlier, X. Blase, and S. Roche, Rev. Mod. Phys. **79**, 677 (2007).
[4] T. W. Odom, J. L. Huang, P. Kim, and C. M. Lieber, J. Phys. Chem. B **104**, 2794 (2000).
[5] A. Rubio, D. Sánchez-Portal, E. Artacho, P. Ordejón, and J. M. Soler, Phys. Rev. Lett. **82**, 3520 (1999).
[6] L. C. Venema, J. W. G. Wildöer, J. W. Janssen, S. J. Tan, H. J. L. Temminck Tuinstra, L. P. Kouwenhoven, and C. Dekker, Science **283**, 52 (1999).
[7] N. Hamada, S. Sawada, and A. Oshiyama, Phys. Rev. Lett. **68**, 1579 (1992).
[8] J. W. Mintmire, B. I. Dunlap, and C. T. White, Phys. Rev. Lett. **68**, 631 (1992).
[9] R. Saito, M. Fujita, G. Dresselhaus, and M. S. Dresselhaus, Appl. Phys. Lett. **60**, 2204 (1992).
[10] B. Sitharaman, K. R. Kissell, K. B. Hartman, L. A. Tran, A. Baikalov, I. Rusakova, Y. Sun, H. A. Khant, S. J. Ludtke, W. Chiu, S. Laus, E. Toth, L. Helm, A. E. Merbach, and L. J. Wilson, Chem. Commun. (Cambridge) **2005**, 3915.
[11] J. Cioslowski, N. Rao, and D. Moncrieff, J. Am. Chem. Soc. **124**, 8485 (2002).
[12] T. Yumura, D. Nozaki, S. Bandow, K. Yoshizawa, and S. Iijima,

J. Am. Chem. Soc. **127**, 11769 (2005); T. Yumura, S. Bandow, K. Yoshizawa, and S. Iijima, J. Phys. Chem. B **108**, 11426 (2004).
[13] A. Rochefort, D. R. Salahub, and P. Avouris, J. Phys. Chem. B **103**, 641 (1999).
[14] D. Lu, Y. Li, S. V. Rotkin, U. Ravaioli, and K. Schulten, Nano Lett. **4**, 2383 (2004).
[15] Z. Zhou, M. Steigerwald, M. Hybertsen, L. Brus, and R. Friesner, J. Am. Chem. Soc. **126**, 3597 (2004).
[16] N. Park, M. Yoon, S. Berber, J. Ihm, E. Osawa, and D. Tomanek, Phys. Rev. Lett. **91**, 237204 (2003).
[17] A. Mananes, F. Duque, A. Ayuela, M. J. Lopez, and J. A. Alonso, Phys. Rev. B **78**, 035432 (2008).
[18] A. J. Du, Y. Chen, G. Q. Lu, and S. C. Smith, Appl. Phys. Lett. **93**, 073101 (2008).
[19] Y. H. Kim, J. Choi, K. Chang, and D. Tomanek, Phys. Rev. B **68**, 125420 (2003).
[20] Y. Higuchi, K. Kusakaba, N. Suzuki, S. Tsuneyuki, J. Yamauchi, K. Akagi, and Y. Yoshimoto, J. Phys.: Condens. Matter **16**, S5689 (2004).
[21] K. Nakada, M. Fujita, G. Dresselhaus, and M. S. Dresselhaus, Phys. Rev. B **54**, 17954 (1996).
[22] Y. Miyamoto, K. Nakada, and M. Fujita, Phys. Rev. B **59**, 9858 (1999).
[23] S. Okada, K. Nadaka, K. Kuwabara, K. Daigoku, and T. Kawai, Phys. Rev. B **74**, 121412(R) (2006).
[24] H. Ohldag, T. Tyliszczak, R. Höhne, D. Spemann, P. Esquinazi, M. Ungureanu, and T. Butz, Phys. Rev. Lett. **98**, 187204 (2007).
[25] P. Esquinazi, D. Spemann, R. Höhne, A. Setzer, K.-H. Han, and T. Butz, Phys. Rev. Lett. **91**, 227201 (2003).
[26] S. Talapatra, P. G. Ganesan, T. Kim, R. Vajtai, M. Huang, M. Shima, G. Ramanath, D. Srivastava, S. C. Deevi, and P. M. Ajayan, Phys. Rev. Lett. **95**, 097201 (2005).
[27] S. S. Alexandre, M. S. C. Mazzoni, and H. Chacham, Phys. Rev. Lett. **100**, 146801 (2008).
[28] Y. W. Son, M. L. Cohen, S. G. Louie, Nature (London) **444**, 347 (2006); **446**, 342 (2007).
[29] O. Hod, V. Barone, J. E. Peralta, and G. E. Scuseria, Nano Lett. **7**, 2295 (2007).
[30] O. Hod, V. Barone, and G. E. Scuseria, Phys. Rev. B **77**, 035411 (2008).
[31] S. A. Wolf, D. D. Awschalom, R. A. Buhrman, J. M. Daughton, S. von Molnar, M. L. Roukes, A. Y. Chtchelkanova, and D. M. Treger, Science **294**, 1488 (2001).
[32] W. Kohn and L. J. Sham, Phys. Rev. **140**, A1133 (1965).
[33] G. Kresse, J. Hafner, Phys. Rev. B **47**, 558 (1993); **49**, 14251 (1994).
[34] G. Kresse and J. Furthmüller, Comput. Mater. Sci. **6**, 15 (1996).
[35] N. D. Mermin, Phys. Rev. **137**, A1441 (1965).
[36] J. P. Perdew and A. Zunger, Phys. Rev. B **23**, 5048 (1981).
[37] D. M. Wood and A. Zunger, J. Phys. A **18**, 1343 (1985).
[38] P. Pulay, Chem. Phys. Lett. **73**, 393 (1980).
[39] P. E. Blöchl, Phys. Rev. B **50**, 17953 (1994).
[40] J. P. Perdew, K. Burke, and M. Ernzerhof, Phys. Rev. Lett. **77**, 3865 (1996).
[41] M. J. Frisch *et al.*, GAUSSIAN03, Revision C.02, Gaussian, Inc., Wallingford, CT, 2004.
[42] J. H. Wu, T. Herrmann, and W. Nolting, Phys. Rev. B **60**, 12226 (1999).
[43] J. Hubbard, Proc. R. Soc. London, Ser. A **276**, 238 (1963).
[44] M. Lee and C. Bruder, Phys. Rev. B **72**, 045353 (2005).
[45] D. Huertas-Hernando, F. Guinea, and A. Brataas, Phys. Rev. B **74**, 155426 (2006).
[46] M. N. Baibich, J. M. Broto, A. Fert, F. Nguyen Van Dau, F. Petroff, P. Etienne, G. Creuzet, A. Friederich, and J. Chazelas, Phys. Rev. Lett. **61**, 2472 (1988).
[47] P. Grünberg, R. Schreiber, Y. Pang, M. B. Brodsky, and H. Sowers, Phys. Rev. Lett. **57**, 2442 (1986).
[48] According to C. W. Chen, M. H. Lee, and J. Clark, Nanotechnology **15**, 1837 (2004), the energy gap of (10,0) SWNTs is 0.8 eV.
[49] M. Fujita, K. Wakabayashi, K. Nakada, and K. Kusakabe, J. Phys. Soc. Jpn. **65**, 1920 (1996).
[50] E. H. Lieb, Phys. Rev. Lett. **62**, 1201 (1989).
[51] Y. Gan, J. Kotakoski, A. V. Krasheninnikov, K. Nordlund, and F. Banhart, New J. Phys. **10**, 023022 (2008); F. Banhart, J. Li, and M. Terrones, Small **1**, 953 (2005).